Available online at www.sciencedirect.com

ScienceDirect

Scripta Materialia 100 (2015) 82–85

Scripta MATERIALIA

www.elsevier.com/locate/scriptamat

Characterization of the residual stresses in spray-formed steels using neutron diffraction

T.L. Lee,[a] J. Mi,[a,*] S.L. Zhao,[b] J.F. Fan,[b] S.Y. Zhang,[c] S. Kabra[c] and P.S. Grant[d]

[a]*School of Engineering, University of Hull, Cottingham Road, Hull HU6 7RX, UK*
[b]*The Advanced Institute, Baosteel Co. Ltd., Shanghai, People's Republic of China*
[c]*ISIS Neutron Source, Science and Technology Facilities Council, Rutherford Appleton Laboratory, Didcot OX11 0QX, UK*
[d]*Department of Materials, University of Oxford, Parks Road, Oxford OX1 3PH, UK*

Received 4 November 2014; revised 24 December 2014; accepted 26 December 2014
Available online 13 January 2015

Neutron diffraction was used to characterize the residual stresses in an as-sprayed tube-shaped steel preform. The measured residual stress distributions were compared with those simulated using finite element method by taking into account the effects of the thermal history, porosity and different phases of the sprayed preform. The porosity was measured using X-ray microcomputed tomography. The study revealed for the first time the correlation between the distribution of porosity and residual stress developed in the as-sprayed preform.

Keywords: Neutron diffraction; Residual stresses; Spray forming; Three-dimensional tomography; Finite element analysis

Porosity is common in spray-formed materials [1], especially at the base and top surface regions of the as-sprayed preforms (up to ~20%) [2], and is detrimental to the mechanical properties [3]. Hot isostatic pressing is often required to remove the porosity before the preform can be further processed or used directly. Porosity has also been shown by finite element (FE) modelling to affect the residual stresses in sprayed materials, especially when a critical porosity threshold is exceeded [4]. The bonding integrity between the particles in the preform and at the preform–substrate interface plays a critical role in determining the material's mechanical properties and performance, while the residual stresses associated with the preform cooling can also become a primary cause of premature failure [5]. Recently, Ristau et al. [6] used FE modelling to study the development of residual stresses in sprayed preforms by taking into account the thermal history during the spray forming and subsequent heat treatment, but stresses were not validated experimentally. Direct measurement of stress development during spray forming is generally not feasible due to the harsh environment and experimental complexity. However, the residual stress can be characterized non-destructively after spraying using diffraction techniques. Ho and Lavernia [7] used laboratory-based X-ray diffraction but, due to the micrometre penetration depth of the X-rays, measurements were confined to the near-surface region [8], which is generally subjected to substantial stress relaxation. Neutron diffraction (ND) offers more capability since neutrons can penetrate most metallic materials up to a few centimetres [9]. The recent development of third-generation neutron strain scanners offers the prospect of at least an order of magnitude improvement in counting times [9], and such scanners have been successfully used to characterize the residual stress in "thick" engineering materials [10]. Until now, there has been no ND characterization of the residual stresses in spray-formed components and how to account for and interpret the link between the as-sprayed porosity and the residual stresses.

In this paper, X-ray microcomputed tomography (μCT) was used to quantify the porosity distribution of an as-sprayed steel preform and ND was used to characterize the residual stress distribution through the preform thickness with varying porosity. The relationship between porosity and residual stresses was studied and interpreted by FE modelling.

An as-sprayed tube-shaped preform was manufactured by Baosteel (China). ASP30 steel was sprayed onto a pre-heated T91 steel tube substrate (773 K and 66 rpm rotation) using a closed-coupled gas atomizer with nitrogen gas at a pressure of 1.3 MPa. The melt pouring temperature was 1843 K and the average melt flow rate was 0.5 kg s^{-1}. The preform was sprayed with multiple passes under the metal spray for 170 s using a substrate horizontal travel velocity of 5 mm s^{-1}. A 10 mm wide and 20 mm thick ring of the spray-formed steel was sectioned from one end of the preform for residual stress measurements. Microstructural

* Corresponding author. Tel.: +44 1482 465670; e-mail: j.mi@hull.ac.uk

http://dx.doi.org/10.1016/j.scriptamat.2014.12.019
1359-6462/

characterization revealed that interfacial bonding was not achieved between the substrate and the preform, and that the preform had two distinct layers (Fig. 1a): a high-density inner layer and a lower-density (porous) outer layer. The dense layer was formed in the first few passes with droplets from the initial hot spray, while the more porous layer developed in subsequent passes under a progressively colder spray because of the reducing melt hydrostatic pressure in the tundish and thus reducing melt flow rate. Samples ($2 \times 2 \times 20$ mm) were cut from the ring and the through-thickness porosity distribution was measured using an X-ray μCT scanner (HMX 160; X-Tek Systems) with a voxel size of $5.93 \times 5.93 \times 5.93$ μm^3. AVIZO v.6.3.1 software was used to segment the 3-D data set.

Residual strains in the ring were measured in the radial (ε_r), hoop (ε_θ) and axial (ε_z) directions using the time-of-flight (TOF) neutron diffractometer at ENGIN-X, ISIS Neutron Source [9]. The sample and ND set-up are shown in Figure 1a. The scan step size was 1 mm and a gauge volume (GV) of $1 \times 4 \times 4$ mm (1 mm in the ε_r direction) was used for ε_θ and ε_z, while $4 \times 4 \times 4$ mm was defined for ε_r. Due to the ε_r scan orientation, the larger GV was necessary to maintain a symmetrical GV shape. It is well documented that a partially filled GV can shift the neutron-weighted centre of gravity (ncog) from the GV geometric centre of gravity (gcog), resulting in artificial peak shifts and pseudo-strains [11]. The GV in the experiment was meticulously positioned in the sample using theodolites to ensure complete filling and any near surface (partially filled GV) measurements were disregarded. Along the scanned path, the effect of porosity distribution in the GV on the shift in the ncog (Fig. 1c) was determined by calculating the centre of mass of the material in the GV and the corresponding pseudo-strains generated due to the ncog shift were determined relative to the detector at $2\theta = 90°$ using [11]:

$$\varepsilon_{P_s} = \frac{\Delta L}{L} + \cot\frac{2\theta}{2} \cdot \frac{\Delta 2\theta}{2} \quad (1)$$

where 2θ and L are the diffraction angle and neutron flight path length from the gcog to the detector, respectively, and $\Delta 2\theta$ and ΔL are their corresponding changes due to the ncog shift. Figure 1b shows that the maximum ncog shift occurred when the GV was in the steep porosity gradient region, with no ncog shift in regions without porosity gradients. The slight ncog shift at the dense region (4–6 mm from interface) was because the GV contained some porosity in the GV vertex region (GV diagonal of 5.66 mm). The calculated maximum compressive pseudo-strain was ~35 με (Fig. 1b) which is about one-fifth of the average ND measurements uncertainty (~170 με). Pseudo-strains due to vertical ncog shifts are much smaller than those due to lateral shifts [11], so were ignored. Hence, it was assumed that the error caused by the pseudo-strains due to porosity did not affect the final stress distribution significantly.

Whole-pattern Rietveld refinements via GSAS [12] were used to obtain the lattice parameters d and phase weight fractions (PWFs) from the TOF diffractograms. The residual strain was calculated using $\varepsilon = (d - d_0)/d_0$, where d_0 is the stress-free lattice parameter. Coupons of dimensions $5 \times 20 \times 30$ mm (20 mm in the ε_r direction) were sectioned from the ring using electrical discharge machining. Annealing heat treatment (1173 K, furnace cooled at 10 K h^{-1} to 973 K, then freely to ambient temperature) was applied to two coupons to obtain stress-free samples for d_0 measurement. However, the heat treatment resulted in the

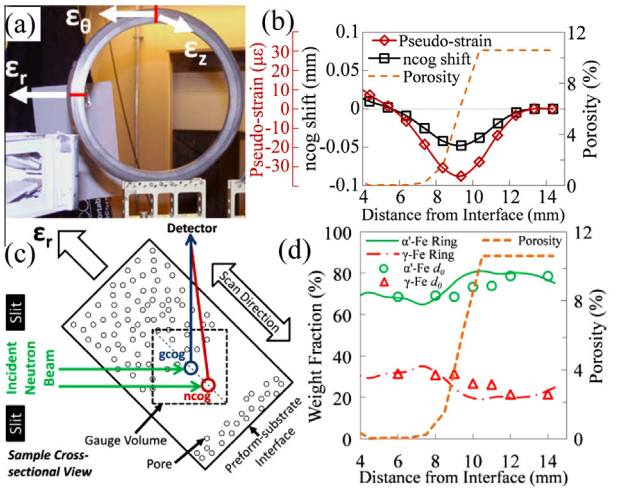

Figure 1. (a) The ND experimental set-up at ENGIN-X showing the etched ring sample, (b) the calculated ncog shift and the corresponding pseudo-strains, (c) a schematic diagram of the neutron beam path scattered from the gcog and ncog and (d) ring and stress-free sample PWF distributions.

decomposition of metastable austenite (γ-Fe) and the as-sprayed phase fractions were no longer representative. Therefore, the as-sprayed coupon was used as the d_0 sample. Figure 1d shows the PWF distributions for the ring and the d_0 coupon, measured using the same scan configuration, indicating the same distributions of martensite (α′-Fe) and γ-Fe in both samples. The measured d_0 values from the coupon were averaged for each phase and used as the d_0 for subsequent estimates of principal residual strains.

The residual strains measured are macrostrains since the GV (= 64 mm^3) was much larger than the length scale of the microstructure or the porosity in the material (typically 10^{-3}–10^{-2} mm^3). Under a condition of elastic deformation, any localized variations in the principal stress direction caused by the free surfaces of the randomly distributed and oriented porosity should be averaged out at this macrolength scale. The arrangement is qualitatively similar to variations of principal strains in non-porous materials with micrometre grains in the form of intergranular stresses, which are assumed to average out in the measurements from a large GV [8]. The corresponding residual stresses, σ_i can be calculated from the measured strains using Hooke's law:

$$\sigma_i = \frac{E}{1+\nu}\left[\varepsilon_i + \frac{\nu}{1-2\nu}(\varepsilon_r + \varepsilon_\theta + \varepsilon_z)\right] \quad (2)$$

where subscript i denotes the respective principal stresses, E is the Young's modulus and $\nu = 0.3$ is the Poisson's ratio. The TOF diffractograms (Fig. 2a) showed that α′-Fe and γ-Fe were the dominant phases, as reported in similar as-sprayed steel alloys [13]. The bulk residual stress, $\sigma_{\alpha'+\gamma}$ can be determined from the phase-specific residual stress using a rule of mixture (ROM) [14]:

$$\sigma_{\alpha'+\gamma} = f_{\alpha'}\sigma_{\alpha'} + (1 - f_{\alpha'})\sigma_\gamma \quad (3)$$

where $f_{\alpha'}$ is the α′-Fe PWF, $\sigma_{\alpha'}$ and σ_γ and are the α′-Fe and γ-Fe phase stress, respectively,which were calculated using Eq. (2), with the Young's modulus of each phase estimated from the corresponding steel, i.e. 200 GPa for α′-Fe and 193 GPa for γ-Fe [15]. Figure 2b shows the residual